HHS Public Access

Author manuscript

Arthritis Rheumatol. Author manuscript; available in PMC 2024 October 01.

Published in final edited form as:

Arthritis Rheumatol. 2023 October ; 75(10): 1831–1841. doi:10.1002/art.42535.

Caspase-1 Enhances TANGO1 Expression to Promote Procollagen Export from the Endoplasmic Reticulum in Systemic Sclerosis Contributing to Fibrosis

Lianne M. Connolly, MS[a], **Caya M. McFalls, MD**[a,b], **Isabelle G. McMahon, BS**[a,c], **Akash M. Bhat, BS**[a], **Carol M. Artlett, PhD**[a]

[a] Department of Microbiology and Immunology, Drexel University College of Medicine, Philadelphia, PA.

[b] Current address: Johns Hopkins Hospital

[c] Current address: ZS Associates, Princeton NJ

Abstract

Objective.—TANGO1 (Transport ANd Golgi Organization protein 1) is a protein that regulates the export of procollagen from the endoplasmic reticulum and has a role in the organization of exit sites for general protein export. What regulates the expression of TANGO1, and its role in fibrosis, is poorly understood, and has never been studied in systemic sclerosis (SSc). We undertook these studies to determine the role for TANGO1 in SSc fibrosis.

Methods.—SSc (n=15) and healthy (n=12) primary fibroblast lung cell lines were investigated for the expression of TANGO1. Histological analyses for TANGO1 were performed on lung biopsies (n=12 SSc and n=8 healthy).

Results.—SSc fibroblasts show increased TANGO1 protein in cultured fibroblasts. TANGO1 colocalizes with α-SMA positive cells in SSc lung tissue and is highly upregulated in the neointima of SSc vessels. TANGO1 expression was dependent on the inflammasome activation of caspase-1. It was also dependent on signaling from the IL-1 and TGF-β receptors. The decrease in TANGO1 downregulated export of larger cargos including collagen, and laminin. Reduced TANGO1 protein had no effect on smaller molecular weight cargoes, however, the secretion of elastin was significantly reduced.

Conclusion.—TANGO1 is markedly increased in SSc fibroblasts and found elevated in lung tissue in association with α-SMA positive cells. TANGO1 expression is driven by inflammasome-dependent caspase-1 activation and is mediated by IL-1 and TGF-β downstream signaling. These observations suggest that during fibrosis, caspase-1 promotes the upregulation of TANGO1, and the organization of ER exits sites, ultimately contributing to procollagen export and fibrosis.

Address Correspondence to: Carol M. Artlett, PhD, Associate Professor, Dept. Microbiology and Immunology, Drexel University College of Medicine, Drexel University, 2900 Queen Lane, Philadelphia PA 19129, carol.artlett@drexelmed.edu.

Competing Interests statement: the authors declare that they have no conflict of interest with these studies.

Keywords

TANGO1; caspase-1; fibrosis; SSc; procollagen export; ER

Introduction

Fibrosis is a chronic, progressive connective tissue pathology. The etiology is often unknown, but it can severely affect quality of life with increased mortality depending on the organ afflicted (1). Myofibroblasts play an active role in fibrosis. These enlarged senescent cells display an expanded endoplasmic reticulum (ER) (2) and are responsible for the bulk of collagen and extracellular matrix deposition during fibrosis.

Systemic sclerosis (SSc) is an autoimmune fibrotic disorder with persistently activated myofibroblasts, which mediate the excessive deposition of collagen and other extracellular matrix proteins (3–6) in the skin, vasculature, and internal organs. In myofibroblasts derived from SSc patients, we previously demonstrated the crucial role for caspase-1 in the deposition of collagen in the tissues (7). Inhibition of caspase-1 abrogated collagen secretion and lowered α-smooth muscle actin (α-SMA) expression (7).

Recent studies identified TANGO1 (Transport ANd Golgi Organization protein 1) in procollagen trafficking from the ER to the Golgi (8). TANGO1 orchestrates the loading of procollagen into growing vesicles, allowing for its export from the ER (9), and organizes ER exit sites (10). There is controversy however, as to how procollagen moves between the ER and Golgi. Several investigators have reported enlarged COPII vesicles are responsible, while others suggest tubular-saccular structures (9, 11, 12). Irrespective as to the mode of export out of the ER, TANGO1 plays a crucial role in this process.

TANGO1 has five isoforms and the two best studied are TANGO1-Long and TANGO1-Short. TANGO1-L has a molecular weight of 213.7 kDa and contains a collagen binding motif whereas TANGO1-S, sized 113.7 kDa, lacks this binding motif. Elegant studies by McCaughey and colleagues (13), show that the disruption of TANGO-L alone does not significantly affect the secretory pathway, while the loss of both the long and short isoforms severely impacts protein secretion. Saito and colleagues (9), found COL7A1 secretion was unaffected by TANGO1 siRNA knockdown in a fibroblast cell line (RDEB/FB/C7) that had been transfected with a COL7A1 plasmid. SAOS2 (osteosarcoma) cell line was also evaluated, and collagen secretion was unaffected by TANGO1 knockdown. In contrast, COL1A1 secretion was affected by siRNA knockdown of TANGO1 in TGF-β1-treated hepatic stellate cells (14). These observations are divergent and may implicate the role for the over expression of TANGO1 during fibrosis and its role in excessive collagen secretion in this pathology.

Considering the recent studies investigating TANGO1 in procollagen export, the regulation of TANGO1 expression is poorly appreciated in fibrosis and has never been studied in SSc. Maiers and colleagues (14), investigated the role for TANGO1 in hepatic fibrosis. They found TGF-β1 to be an important cytokine that increased the expression of TANGO1 via XBP1s (14). Their findings are important and set the stage for further investigation of

this protein in other fibrotic disorders. As TANGO1 organizes ER exit sites and is one of the crucial proteins in the export of procollagen, we undertook these analyses to find the relevance of TANGO1 in fibroblasts derived from SSc fibrotic lesions and to determine if its expression was dependent on caspase-1 activation. A better understanding of this process and the factors controlling the expression of TANGO1, and thus the export of procollagen from the ER during fibrosis, could potentially identify novel therapeutic targets for not only SSc, but other fibrotic diseases.

Materials and Methods.

Fibroblast Cell lines.

All patients in this study fulfilled the criteria established for the classification of SSc (15). Human studies were approved by the Institutional Review Boards at Drexel University and the University of Pittsburgh. Primary human fibroblast cell lines were derived from the lungs of SSc patients (n=15) or from healthy individuals (n=12) who had died of an unrelated event (e.g., trauma, car/motorcycle accidents, CVA, etc.), and were a kind gift from Dr. Feghali-Bostwick at the Medical University of South Carolina. Of the patients with SSc, all were undergoing lung transplant at the University of Pittsburgh; three were male, ten were female, and two were unknown. Six had diffuse disease, five had limited disease, and four were unclassified for their subset. Nine were Caucasian, one Asian, one African American, and four were unclassified for their race. Of the healthy individuals, two were male and ten were female. Patients were aged 27–56 (median 43) years and healthy individuals were aged 26–76 (median 43) years.

Cell Culture.

Primary cell lines at low passage (<5) were cultured in Dulbecco's Modified Eagles Medium (DMEM) supplemented with 10% FBS and antibiotics and were grown at 37°C with 5% CO_2 in a humid atmosphere. Healthy or SSc fibroblasts were seeded at a density of 28,000 cells/cm^2 growth area in DMEM and allowed to adhere overnight. Media was changed and then the cells were treated with either 20μM Z-YVAD-FMK (YVAD, ApexBio), 2μg/ml IL-1RA (Tonbo Biosciences), or 10μM ALK5 Inhibitor II hydrochloride (ALK5, Cayman Chemical) for 48 h. These inhibitors did not affect cell growth (Figure 6C). Media was harvested and cell pellets lysed with NP40 lysis buffer to extract protein. All samples were stored at −80°C until analyzed.

siRNA Studies.

siRNA nucleotides for TANGO1 and caspase-1 were purchased from Santa Cruz Biotechnology. The day prior to transfection, 500,000 fibroblasts were seeded in 10% FBS/DMEM into 60 mm dishes and allowed to adhere overnight. Transfections were performed according to the RNAiMax protocol (ThermoFisher). Briefly, 110pmol siRNA was added to 250μl serum free/antibiotic free media then combined with 250μl of serum free/antibiotic free media containing 15μl RNAiMax reagent and incubated at room temp for 5 min. The fibroblasts were given fresh media complete with 10% FBS and antibiotics with the siRNA. The siRNA procedure was repeated the next day and protein from the cells recovered 24h after the second treatment.

Immunoblotting.

Fifty-micrograms of total cell lysate was separated on 8% SDS PAGE gels for 150 mins at 120 volts on ice using the discontinuous buffer system (16). The separated proteins were transferred to nitrocellulose using Towbin buffer (pH 8.3) for 75 min at 30 volts on ice. The nitrocellulose was stained with Ponceau S for 10 min and briefly washed to clarify the bands, then scanned and total protein quantified. Tubulin was initially used as a loading control for secreted proteins; however, we found it to be dependent on TANGO1 and therefore secreted proteins were normalized to total protein in each lane stained with Ponceau S. Ponceau S was removed with three washes in Tris buffered saline (TBS) and then non-specific binding sites were blocked with 5% skim milk in TBS for 3h. Membranes were incubated overnight with the primary antibody diluted in 3% BSA/TBS at 4°C on a rocker. Primary antibodies used for immunoblotting were TANGO1 (1:1000, Proteintech, Cat#17481–1-AP-150UL), COL1A1 (1:2000 Cell Signaling Cat#72026S), caspase-1 (1:1000 Santa Cruz Biotechnology Cat#sc-392736), laminin (1:1000, Abcam Cat#ab11575), fibronectin (1:1000, Abcam Cat#ab2413), elastin (1:1000, Santa Cruz Biotechnology, Cat#sc-166543), HSP90 (1:1000, ENZO Cat#ADI-SPA-830-D), and β-actin (1:2000, Cell Signaling Cat#4970S). Unbound antibody was removed from the membranes in three washes of TBS and incubated with donkey-anti-rabbit-HRP (Jackson ImmunoResearch 1:2000 for all antibodies except β-actin which was diluted 1:4000) at room temp for 3h, washed with three changes of TBS and the HRP signal developed with SuperSignal West Dura Extended Duration Substrate (ThermoFisher Scientific). The intensity of the signal on the nitrocellulose was digitized using the ImageQuant LAS4000 (GE Healthcare), and band densities measured using ImageQuant LT 7.0 (GE Healthcare) software.

Column fractionation.

$1X10^6$ SSc and healthy fibroblasts at passage 4 were cultured for 48 h and media was collected and stored at −80°C until assayed. One milliliter of media was size fractionated through a 100 kDa cut off column at 2200 rpm for 10 min at 4°C. Media retained in the upper portion of the column (>100 kDa) and in the lower portion of the column (<100 kDa) were collected and assayed for protein concentration using the bicinchoninic acid assay.

Sirius Red.

From the samples used in the column fractionation, 500μl of culture media was incubated with an equal volume of 1% sirius red, shaken for 30 sec, and placed on ice for 60 min, then centrifuged at 7000g for 10 min. The supernatant was carefully removed, and the pellets washed with 1M acetic acid with centrifugation three times or until the supernatant was faintly pink. The sirius red was released from the pellets with 2M NaOH by vortexing and the optical density measured at 570 nm with an Infinite M $Nano^+$ (Tecan) plate reader.

Immunofluorescence.

Sections from paraffin embedded lung biopsies (n=12) from patients with SSc and (n=8) healthy lung tissue were obtained from Dr Feghali-Bostwick and deparaffinized in two changes of ethanol and two changes of xylene (20 min each), then hydrated in PBS. Antigen

retrieval was performed in 10 mM citrate buffer pH 6.0 at 100°C for 30 min, then blocked with 5% goat serum (Jackson ImmunoResearch) for 20 min. TANGO1 diluted 1:100 in PBS (Proteintech Cat#17481–1-AP-150UL) was applied to the slides for 60 min. Unbound antibody was removed with three washes of PBS, then incubated with goat-anti-rabbit-Cy3 (Jackson ImmunoResearch, Cat#111–165-045) diluted 1:400 in PBS for 60 min. Slides were washed then immediately stained with α-SMA (BioLegend Cat#904601) diluted 1:200 in PBS for 60 min, washed in three changes of PBS, and incubated with goat-anti-mouse-Cy2 diluted 1:500 for 60 min, washed as described, and mounted in SlowFade Gold antifade reagent with DAPI, viewed and photographed.

Statistical analyses

Statistical analyses were performed with GraphPad Prism 9.0. For comparisons between two groups (healthy fibroblasts vs. SSc fibroblasts), two-tailed unpaired t-tests were conducted. For analyses of three or more groups, one-way ANOVA was used, with Dunnet's multiple comparison test when the experimental groups were compared to the control group. Tukey's multiple comparison test was used when statistical analyses was performed between all the groups. Adjusted p values less than 0.05 were considered significant.

Results

TANGO1 is elevated in SSc.

During fibrosis we expect an increase in protein transport through the ER, including larger sized proteins such as procollagen. Because TANGO1 organizes ER exit sites (17) and is involved in procollagen export (9, 18), we reasoned that there could be an increase in TANGO1 protein in fibroblasts derived from patients with SSc. Using immunoblotting, we found increased protein for TANGO1-L and TANGO1-S in SSc lung fibroblasts compared to healthy lung fibroblasts (Figure 1).

We immunostained cultured SSc and healthy lung fibroblasts for TANGO1 and found that the SSc fibroblasts had enlarged TANGO1 positive green aggregated punctates while punctates in the healthy fibroblasts were smaller and diffuse (Figure 2A). In lung tissues from SSc patients stained for TANGO1 (red) and α-SMA (green), we noted strong colocalization of the two markers in vessel walls, and if present, in the neointima, and in sheets of α-SMA positive cells (Figure 2B). Control tissues were negative for this colocalization (Figure 2B), although the occasional TANGO1 positive cell was noted.

During fibrosis, TANGO1-L and TANGO1-S are dependent on caspase-1 activity and its downstream signaling products.

We previously showed the role for caspase-1 in SSc fibrosis (7) and wanted to determine if it had a role in TANGO1 expression. We found that inhibition of caspase-1 activity with YVAD in SSc fibroblasts significantly lowered both isoforms of TANGO1 (Figure 3A–C). Furthermore, knowing that caspase-1 causes the maturation of IL-1β and that YVAD significantly reduces the secretion of IL-1β by SSc fibroblasts (7), we wanted to determine if IL-1 had a role in TANGO1 expression. TGF-β1 is also an important cytokine in SSc and was previously shown to induce TANGO1 expression (14). We therefore blocked the

engagement of IL-1 with its receptor using IL-1RA and blocked TGF-β receptor signaling with ALK5 in SSc fibroblasts. We showed that both TANGO1-L and TANGO1-S were significantly lowered in the presence of IL-1RA and ALK5 (Figure 3A–C). We then investigated intracellular and extracellular COL1A1 (Figures 3A, 3D–E). We show that intracellular COL1A1 was decreased with YVAD and ALK5 and we also saw an overall reduction in the secretion of COL1A1 into the media. In contrast, we saw that while IL-1RA decreased TANGO1 expression and reduced secreted COL1A1 (Figures 3A and 3E), there was a corresponding increase in intracellular COL1A1 (Figures 3A and 3D). To ensure that the decrease of TANGO1 did not cause ER stress and cell death because collagen could not be exported out of the ER, we performed a proliferation assay and found that there was no loss of cells over the 48 h (Figure 6C). The overall lowered TANGO1-L and TANGO1-S protein had a profound effect on collagen secretion suggesting that TANGO1 plays an important role in SSc fibrosis.

During fibrosis TANGO1 expression requires caspase-1.

YVAD inhibits caspase-1 but is also known to have some activity against caspase-4 and caspase-5. Therefore, we wanted to specifically ascertain the relevance for caspase-1 in TANGO1 expression in SSc fibrosis. We performed siRNA targeting caspase-1, and in these studies we also performed siRNA to target TANGO1. We showed that the specific targeting of caspase-1 significantly lowered TANGO1 protein (Figure 4A–B). As expected, we also showed that targeting TANGO1 with siRNA significantly reduced the expression of this protein (Figure 4A–B). We confirmed our earlier findings (7), that caspase-1 is required for collagen secretion and show that COL1A1 was significantly reduced when caspase-1 siRNA is employed (Figure 4C–D). In addition, when TANGO1 protein is reduced with siRNA, COL1A1 was also significantly lowered (Figure 4C–D). We then assessed total collagen secreted into the media and found that with both caspase-1 siRNA and TANGO1 siRNA it was lowered (Figure 4E). We did note however, that with knockdown of TANGO1, COL1A1 and total collagen secretion was not completely abolished (Figure 4C–E).

SSc fibroblasts secrete more higher molecular weight proteins, and this is dependent on TANGO1.

It has been suggested that TANGO1 is involved in the secretion of other high molecular weight proteins besides procollagen (19–22), and may also play a role in the secretion of low molecular weight proteins as well (13, 17). Media from SSc and healthy fibroblasts cultured at low passage were size fractionated across a 100kDa cut off column and total protein measured. We found fibroblasts derived from patients with SSc secreted significantly more of the higher molecular weight proteins (>100kDa) compared to healthy fibroblasts (Figure 5A), while the concentrations of proteins in the <100kDa fraction were not significantly different between the two groups (Figure 5B). From the >100kDa fraction, we found that the concentration of total collagen was also significantly elevated in SSc fractionated media (Figure 5C). In the >100kDa fraction we saw a corresponding increase in the secretion of COL1A1 (Figure 5D).

We next fractionated media from SSc fibroblasts after they were treated with YVAD, IL-1RA, or ALK5 (Figure 6). We determined total protein in the >100kDa fraction and

found it significantly reduced with the three inhibitors (Figure 6A). In the <100kDa fraction there was no significant difference with the three inhibitors for total protein recovered (Figure 6B), although we note in Figures 3A–C that TANGO1 is significantly decreased by all three inhibitors but not completely abolished. In addition to collagen, we assessed other specific proteins increased during fibrosis including laminin, fibronectin, elastin, and HSP90. We found the secretion of laminin (Figure 6C and 6E) and elastin (Figure 6C and 6F) were reduced with YVAD, IL-1RA, and ALK5. However, fibronectin and HSP90 were not lowered (Figure 6C and 6G).

Discussion.

TANGO1 is a key protein in the export of procollagen, in part because it spatially organizes ER exit sites, but also because it has a binding motif that recruits the procollagen chaperone HSP47. Elegant studies by Liu and colleagues (17), demonstrate that while TANGO1 spatially organizes ER exit sites for protein export and may facilitate the formation of canals allowing for the flow of nascent protein from the ER to the Golgi, they also found that the complete loss of TANGO1 causes smaller ER exit sites and uncoupling of the ER from the Golgi. They additionally suggested that ER-Golgi contact might be a more efficient process whereby large proteins move out of the ER and into the Golgi. In support of this hypothesis, McCaughey and colleagues (23), proposed a short loop model for ER to Golgi trafficking of procollagen. McCaughey and colleagues (13), later proved that TANGO1 has a general role in the secretory pathway. They showed the disruption of TANGO1-L had a minor effect on protein secretion, while the complete loss of both TANGO1-L and TANGO1-S had major defects in cell organization and secretion.

Here we analyzed fibrotic lung fibroblasts and biopsies from patients with SSc. Our results are consistent with the highly upregulated nature of this ER export process during fibrosis. We demonstrate increased expression of the long and short isoforms of TANGO1 protein suggestive of the increased intracellular movement of procollagen and other proteins from the ER to Golgi in SSc fibroblasts. Histological analyses showed TANGO1 to co-localize within α-SMA positive cells in SSc biopsies but was not found in α-SMA positive cells in controls.

We also show that the elevated expression of both TANGO1-L and TANGO1-S is dependent on caspase-1 activity and its downstream signaling products such as IL-1 and TGF-β. Intriguingly, when caspase-1 was inhibited with YVAD, this lowered both TANGO1 protein and intracellular COL1A1. When ALK5 was used, this lowered intracellular COL1A1 protein by blocking TGF-β receptor-mediated COL1A1 expression, and as a result, decreased TANGO1 protein, likely because the profibrotic pressure to export COL1A1 was reduced. Alternatively, it is possible that decreased intracellular COL1A1 led to decreased available COL1A1 for export, thus reducing the burden on TANGO1 and lowering the protein level by other mechanisms. When IL-1RA was used, this decreased both the long and short forms of TANGO1 and extracellular COL1A1 was decreased. However, intracellular COL1A1 increased, suggesting that COL1A1 was not being actively exported due to the lowered TANGO1. This observation also suggests that there are other mechanisms that regulate the export of COL1A1 from the ER during fibrosis. MTT studies showed no

cell loss and therefore the increased intracellular collagen did not cause ER stress (Figure 6C).

Using siRNA, we further define that in fibrosis, TANGO1 protein is dependent on caspase-1, and as a result there was significant reduction in TANGO1 protein when siRNA was used (Figure 4). We also show in these studies that because TANGO1 is reduced with caspase-1 siRNA, there is a corresponding reduction in extracellular COL1A1 and total secreted collagen. Using TANGO1 siRNA, we also saw a significant decrease in TANGO1 protein in the cell lysates and reduced extracellular COL1A1 and total secreted collagen. We confirm Saito's findings (9), who found that knockdown of TANGO1 reduced the secretion of collagen. However, they studied the rarer COL7 molecule and found it reduced by 80%. In our studies, we found a 64% and 86% reduction in extracellular COL1A1 with caspase-1 siRNA and TANGO1 siRNA treated SSc fibroblasts, respectively. Secretion of total extracellular collagen, conversely, was decreased by 28% and 30%, respectively (Figure 4E). This suggests that during fibrosis, there are likely other proteins involved in procollagen export, or that TANGO1 does not bind all procollagens, and some are released independent of TANGO1 via other mechanisms. These observations also suggest that inhibition of TANGO1 might be a useful therapeutic approach to control fibrosis as some collagen can still be secreted. We speculate that this would be advantageous in fibrosis especially if the interaction between TANGO1-L and HSP47 is inhibited as this would reduce the amount of procollagen recruited and exported via COPII vesicles.

We also demonstrate the novel finding that during SSc-mediated fibrosis the mechanistic flow of nascent cargo out of the ER necessitated by TANGO1 is dependent on caspase-1 activity. Caspase-1 is known for its ability to regulate unconventional protein secretion e.g., the cleavage of pro-IL-1β for secretion. Here we demonstrate that during fibrosis, the upregulation of TANGO1 expression is dependent on caspase-1, which is mediated by downstream signaling from the IL-1 and TGF-β receptors (Figure 3). These observations provide further crucial evidence that caspase-1 plays a role in conventional secretion by upregulating TANGO1 expression and as a result mediating the organization of ER exit sites.

TGF-β1 and IL-1β demonstrate substantial cross talk between their respective pathways (24) and both cytokines are involved in SSc fibrosis (7, 25–27). In the normal context of wound healing, once the wound is closed, IL-1 downregulates TGF-β1. However, the mechanism behind fibrosis is complex, poorly understood, and there is no "wound" *per se*. Serum IL-1β levels are unreliable indicators for the role of this cytokine in fibrosis and many inflammatory diseases (28) as the effects can be localized. However, the long term exposure of IL-1β enhances TGF-β1 signaling (29). The spectrum of diseases caused by IL-1 includes a vast array of hereditary and non-hereditary pathologies that range from systemic to tissue restricted conditions. Our findings suggest that IL-1 plays a significant role upregulating collagen production during fibrosis (7). Supporting this notion, the literature is replete with evidence for the role of IL-1 in fibrotic disorders in both human (30–33) and animal models (25, 34). While we investigated two cytokines, it is likely that other profibrotic molecules, e.g., IL-6 (35), PDGF (36), among others might stimulate the expression of TANGO1

directly, or activate the transcription of TANGO1 indirectly because of the increased burden of procollagen in the ER. Further studies are warranted to prove this hypothesis.

Considering these observations, we studied the secretion of high molecular weight protein (>100 kDa) versus low molecular weight protein (<100kDa) in the media from SSc fibroblasts. SSc fibroblasts secreted significantly more of the high molecular weight proteins than control fibroblasts (Figure 5A), but there were no differences between SSc and controls with respect to low molecular proteins (Figure 5B). We also found that the high molecular weight proteins were significantly lowered with the three inhibitors (Figure 6A), while the low molecular weight fraction had no significant changes (Figure 5B). In our studies, we have not entirely depleted TANGO1 in the fibroblasts, but we show there is approximately 60% reduction in TANGO1-L and 75% reduction in TANGO1-S with YVAD, IL-1RA and ALK5 (Figure 3B and 3C).

Other cargoes are known to be reliant on TANGO1 for their export, including perlecan (19), SPARC (20), tiggrin (21), and laminin (19, 22). We found proteins in the lower molecular weight fraction were minimally affected when TANGO1 was reduced (Figure 6B). This observation was unexpected given that Liu and colleagues (17) and McCaughey and colleagues (13) show that the complete loss of TANGO1 also causes decreased secretion of low molecular weight proteins and severely affects general protein secretion. We speculate that the remaining TANGO1 protein was sufficient for general protein secretion and had a minimal effect on the low molecular weight fraction. However, we did not test for every extracellular matrix protein in this fraction, we did find elastin to be significantly decreased. We speculate that the decrease in elastin when TANGO1 is suppressed might suggest the recruitment of specific extracellular matrix proteins along with the collagen molecules during fibrosis. We also investigated the chaperone HSP90 as it is elevated in SSc and released into the surrounding tissues (37). In contrast, we did not find the heat shock protein HSP90 to be decreased. HSP90 is involved in the secretion of leaderless proteins via liposomes (38) and not via COPII vesicles. This may explain why the protein was not decreased when TANGO1 was lowered. Overall, it appears that the secretion of many other proteins in the low molecular weight fraction stays unaltered and is likely due to two distinct types of ER to Golgi cargo flow: bulk flow and the flow of specifically sorted cargo. Bulk flow includes many smaller soluble proteins that are not actively sorted. These proteins are present in the ER and not actively loaded into COPII vesicles but found inside vesicles when they bud off. The transport of specifically sorted cargo (larger proteins and some smaller ones like elastin) appears to be a more controlled process because they must interact with adaptor proteins for their recruitment into the COPII vesicle.

SSc is a rheumatologic disease with significant clinical and phenotypic variability, so identifying pathways and key mediators of disease can be difficult. Here, we show for the first time that TANGO1 is highly upregulated in diseased fibroblasts derived from SSc patients and is colocalized with α-SMA in lung tissues. We also show that this upregulation is dependent on inflammasome activation of caspase-1 and the downstream cytokines IL-1 and TGF-β. It is likely that in other fibrotic disorders, TANGO1 is also elevated and plays a prominent role in the export of procollagen. Targeting this pathway to disrupt the export

of procollagen and potentially other higher molecular weight proteins out of the ER may identify novel and effective therapeutic inhibitors of fibrosis.

Funding:

This work was supported by the National Institutes of Health R21AR073947 to CMA and the Scleroderma Foundation to CMA. Funding was also from the National Scleroderma Foundation.

References

1. Poudel DR, Jayakumar D, Danve A, Sehra ST, Derk CT. Determinants of mortality in systemic sclerosis: a focused review. Rheum Int. 2018;38:1847–58.
2. Baek HA, Kim do S, Park HS, Jang KY, Kang MJ, Lee DG, et al. Involvement of endoplasmic reticulum stress in myofibroblastic differentiation of lung fibroblasts. Am J Respir Cell Molec Biol. 2012;46:731–9. [PubMed: 21852685]
3. Varga J, Abraham D. Systemic sclerosis: a prototypic multisystem fibrotic disorder. J Clin Invest. 2007;117:557–67. [PubMed: 17332883]
4. Abraham DJ, Eckes B, Rajkumar V, Krieg T. New developments in fibroblast and myofibroblast biology: implications for fibrosis and scleroderma. Curr Rheum Rep. 2007;9:136–43.
5. Tomasek JJ, Gabbiani G, Hinz B, Chaponnier C, Brown RA. Myofibroblasts and mechano-regulation of connective tissue remodelling. Nat Rev. 2002;3:349–63.
6. Kirk TZ, Mark ME, Chua CC, Chua BH, Mayes MD. Myofibroblasts from scleroderma skin synthesize elevated levels of collagen and tissue inhibitor of metalloproteinase (TIMP-1) with two forms of TIMP-1. J Biol Chem. 1995;270:3423–8. [PubMed: 7852429]
7. Artlett CM, Sassi-Gaha S, Rieger JL, Boesteanu AC, Feghali-Bostwick CA, Katsikis PD. The inflammasome activating caspase-1 mediates fibrosis and myofibroblast differentiation in systemic sclerosis. Arthritis Rheum. 2011;63:3563–74. [PubMed: 21792841]
8. Saito K, Yamashiro K, Ichikawa Y, Erlmann P, Kontani K, Malhotra V, et al. cTAGE5 mediates collagen secretion through interaction with TANGO1 at endoplasmic reticulum exit sites. Molec Biol Cell. 2011;22:2301–8. [PubMed: 21525241]
9. Saito K, Chen M, Bard F, Chen S, Zhou H, Woodley D, et al. TANGO1 facilitates cargo loading at endoplasmic reticulum exit sites. Cell. 2009;136:891–902. [PubMed: 19269366]
10. Saito K, Maeda M. Not just a cargo receptor for large cargoes; an emerging role of TANGO1 as an organizer of ER exit sites. J Biochem. 2019;166:115–9. [PubMed: 31098622]
11. Ma W, Goldberg J. TANGO1/cTAGE5 receptor as a polyvalent template for assembly of large COPII coats. Proc Natl Acad Sci USA. 2016;113:10061–6. [PubMed: 27551091]
12. Bonfanti L, Mironov AA Jr., Martínez-Menárguez JA, Martella O, Fusella A, Baldassarre M, et al. Procollagen traverses the Golgi stack without leaving the lumen of cisternae: evidence for cisternal maturation. Cell. 1998;95:993–1003. [PubMed: 9875853]
13. McCaughey J, Stevenson NL, Mantell JM, Neal CR, Paterson A, Heesom K, et al. A general role for TANGO1, encoded by MIA3, in secretory pathway organization and function. J Cell Sci. 2021;134: jcs259075. [PubMed: 34350936]
14. Maiers JL, Kostallari E, Mushref M, deAssuncao TM, Li H, Jalan-Sakrikar N, et al. The unfolded protein response mediates fibrogenesis and collagen I secretion through regulating TANGO1 in mice. Hepatology. 2017;65:983–98. [PubMed: 28039913]
15. van den Hoogen F, Khanna D, Fransen J, Johnson SR, Baron M, Tyndall A, et al. 2013 classification criteria for systemic sclerosis: an American college of rheumatology/European league against rheumatism collaborative initiative. Ann Rheum Dis. 2013;72:1747–55. [PubMed: 24092682]
16. Laemmli UK. Cleavage of structural proteins during the assembly of the head of bacteriophage T4. Nature. 1970;227:680–5. [PubMed: 5432063]
17. Liu M, Feng Z, Ke H, Liu Y, Sun T, Dai J, et al. Tango1 spatially organizes ER exit sites to control ER export. J Cell Biol. 2017;216:1035–49. [PubMed: 28280122]

18. Santos AJ, Raote I, Scarpa M, Brouwers N, Malhotra V. TANGO1 recruits ERGIC membranes to the endoplasmic reticulum for procollagen export. eLife. 2015;4.
19. Lerner DW, McCoy D, Isabella AJ, Mahowald AP, Gerlach GF, Chaudhry TA, et al. A Rab10-dependent mechanism for polarized basement membrane secretion during organ morphogenesis. Developmental cell. 2013;24:159–68. [PubMed: 23369713]
20. Tiwari P, Kumar A, Das RN, Malhotra V, VijayRaghavan K. A Tendon Cell Specific RNAi Screen Reveals Novel Candidates Essential for Muscle Tendon Interaction. PLoS One. 2015;10:e0140976. [PubMed: 26488612]
21. Zhang L, Syed ZA, van Dijk Hard I, Lim JM, Wells L, Ten Hagen KG. O-glycosylation regulates polarized secretion by modulating Tango1 stability. Proc Natl Acad Sci USA. 2014;111:7296–301. [PubMed: 24799692]
22. Petley-Ragan LM, Ardiel EL, Rankin CH, Auld VJ. Accumulation of Laminin Monomers in Drosophila Glia Leads to Glial Endoplasmic Reticulum Stress and Disrupted Larval Locomotion. J Neurosci. 2016;36:1151–64. [PubMed: 26818504]
23. McCaughey J, Stevenson NL, Cross S, Stephens DJ. ER-to-Golgi trafficking of procollagen in the absence of large carriers. J Cell Biol. 2019;218:929–48. [PubMed: 30587510]
24. Lu T, Tian L, Han Y, Vogelbaum M, Stark GR. Dose-dependent cross-talk between the transforming growth factor-beta and interleukin-1 signaling pathways. Proc Natl Acad Sci USA. 2007;104:4365–70. [PubMed: 17360530]
25. Gasse P, Mary C, Guenon I, Noulin N, Charron S, Schnyder-Candrian S, et al. IL-1R1/MyD88 signaling and the inflammasome are essential in pulmonary inflammation and fibrosis in mice. J Clin Invest. 2007;117:3786–99. [PubMed: 17992263]
26. Gasse P, Riteau N, Vacher R, Michel ML, Fautrel A, di Padova F, et al. IL-1 and IL-23 mediate early IL-17A production in pulmonary inflammation leading to late fibrosis. PLoS One. 2011;6:e23185. [PubMed: 21858022]
27. Ghosh AK, Yuan W, Mori Y, Varga J. Smad-dependent stimulation of type I collagen gene expression in human skin fibroblasts by TGF-beta involves functional cooperation with p300/CBP transcriptional coactivators. Oncogene. 2000;19:3546–55. [PubMed: 10918613]
28. Allantaz F, Chaussabel D, Banchereau J, Pascual V. Microarray-based identification of novel biomarkers in IL-1-mediated diseases. Curr Opin Immunol. 2007;19:623–32. [PubMed: 18036805]
29. Luo DD, Fielding C, Phillips A, Fraser D. Interleukin-1 beta regulates proximal tubular cell transforming growth factor beta-1 signalling. Nephrol Dial Transplant. 2009;24:2655–65. [PubMed: 19420104]
30. Lonnemann G, Engler-Blum G, Muller GA, Koch KM, Dinarello CA. Cytokines in human renal interstitial fibrosis. II. Intrinsic interleukin (IL)-1 synthesis and IL-1-dependent production of IL-6 and IL-8 by cultured kidney fibroblasts. Kidney Int. 1995;47:845–54. [PubMed: 7752583]
31. Aouba A, Georgin-Lavialle S, Pagnoux C, Martin Silva N, Renand A, Galateau-Salle F, et al. Rationale and efficacy of interleukin-1 targeting in Erdheim-Chester disease. Blood. 2010;116:4070–6. [PubMed: 20724540]
32. Mikuniya T, Nagai S, Shimoji T, Takeuchi M, Morita K, Mio T, et al. Quantitative evaluation of the IL-1 beta and IL-1 receptor antagonist obtained from BALF macrophages in patients with interstitial lung diseases. Sarcoid Vasc Diffuse Lung Dis. 1997;14:39–45.
33. Hughes FM Jr., Sexton SJ, Jin H, Govada V, Purves JT. Bladder fibrosis during outlet obstruction is triggered through the NLRP3 inflammasome and the production of IL-1beta. Am J Physiol Renal Physiol. 2017:ajprenal.00128.2017.
34. Lan HY, Nikolic-Paterson DJ, Mu W, Vannice JL, Atkins RC. Interleukin-1 receptor antagonist halts the progression of established crescentic glomerulonephritis in the rat. Kidney Int. 1995;47:1303–9. [PubMed: 7637259]
35. Abdel-Magied RA, Kamel SR, Said AF, Ali HM, Abdel Gawad EA, Moussa MM. Serum interleukin-6 in systemic sclerosis and its correlation with disease parameters and cardiopulmonary involvement. Sarcoid Vasc Diffuse Lung Dis 2016;33:321–30.
36. Overbeek MJ, Boonstra A, Voskuyl AE, Vonk MC, Vonk-Noordegraaf A, van Berkel MP, et al. Platelet-derived growth factor receptor-beta and epidermal growth factor receptor in pulmonary

vasculature of systemic sclerosis-associated pulmonary arterial hypertension versus idiopathic pulmonary arterial hypertension and pulmonary veno-occlusive disease: a case-control study. Arthritis Res Ther. 2011;13:R61. [PubMed: 21492463]

37. RuizdelRio J, Muñoz P, Carreira P, Maestro D, Pablos JL, Palanca A, et al. Profibrotic Role of Inducible Heat Shock Protein 90α Isoform in Systemic Sclerosis. J Immunol. 2022;209:38–48. [PubMed: 35715007]
38. Zhang M, Liu L, Lin X, Wang Y, Li Y, Guo Q, et al. A Translocation Pathway for Vesicle-Mediated Unconventional Protein Secretion. Cell. 2020;181:637–52.e15. [PubMed: 32272059]

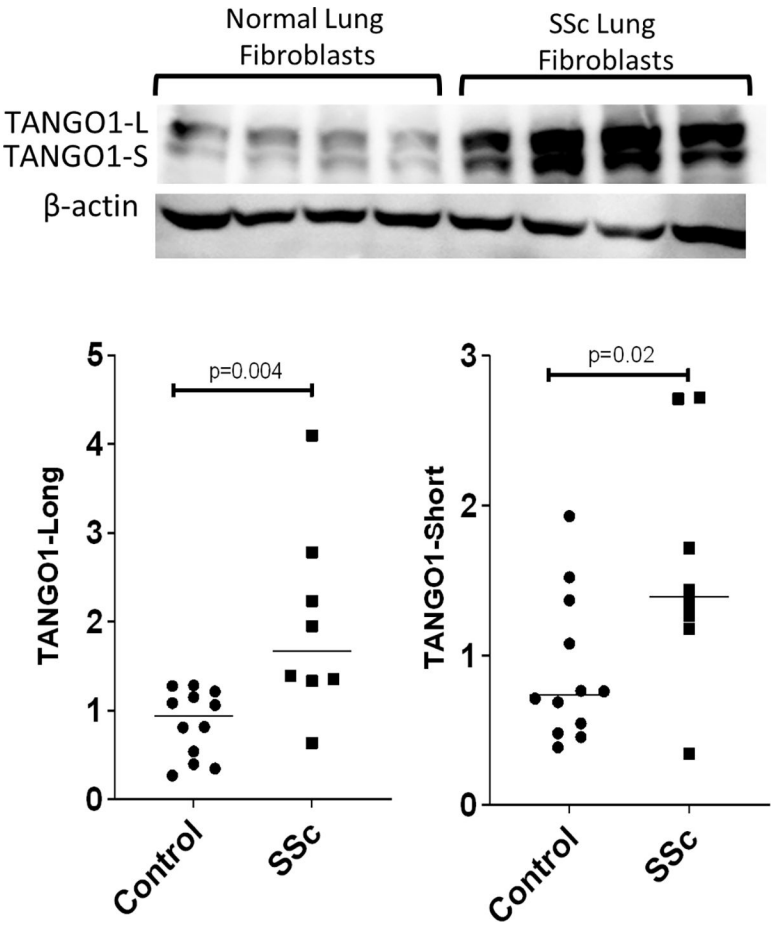

Figure 1. TANGO1 is elevated in SSc lung fibroblasts.

A: A representative immunoblot for TANGO1 showing expression in healthy and SSc fibroblasts. The density of TANGO1-Long (TANGO1-L) and TANGO1-Short (TANGO1-S) bands are presented graphically and individual data values are presented. Data is compiled from n=12 healthy and n=8 SSc fibroblast cell lines. Statistical analyses: two tailed unpaired t-test.

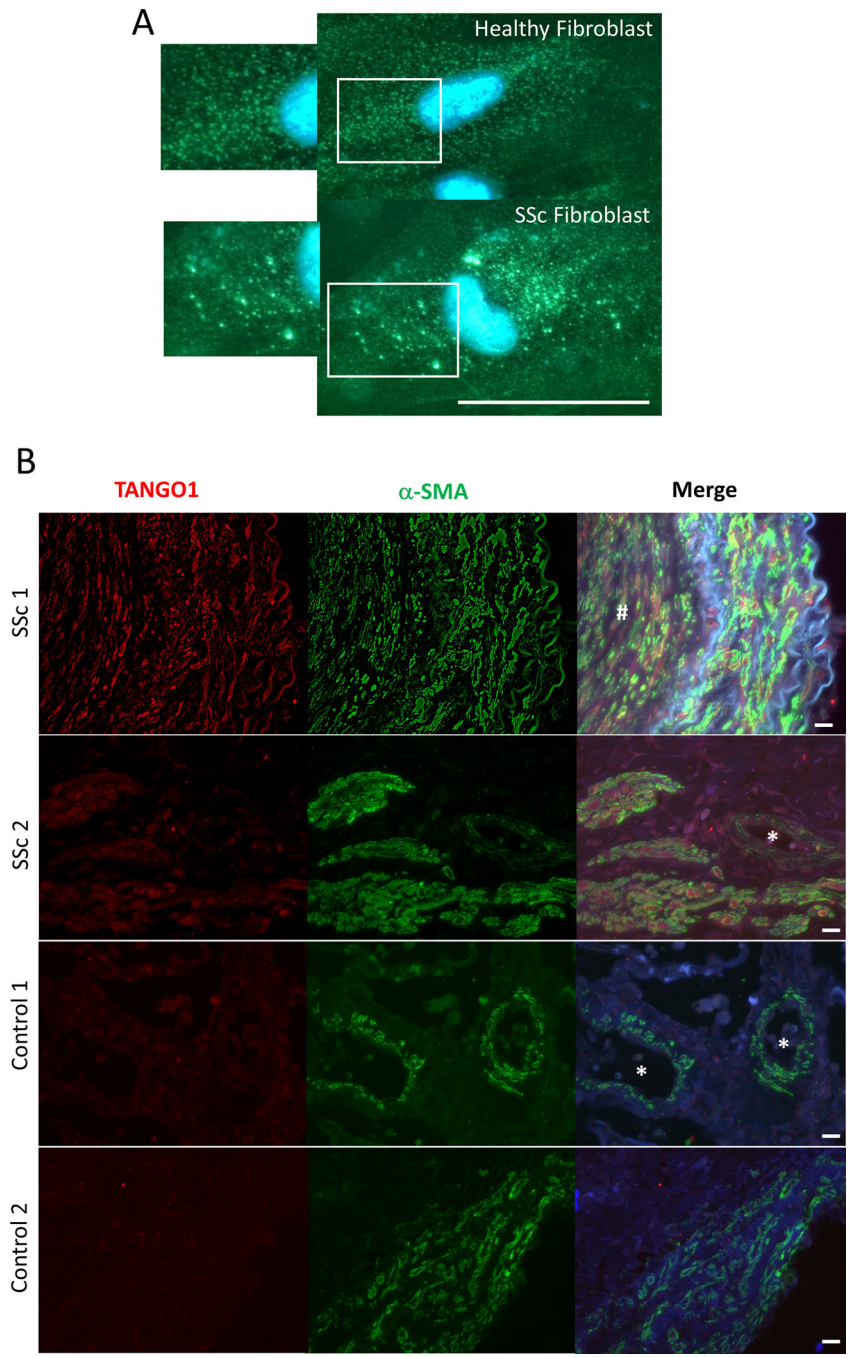

Figure 2. Localization of TANGO1 in SSc tissues correlates with myofibroblasts and is especially elevated in neointima of vessels.

A: Immunofluorescence staining of cultured fibroblasts for TANGO1 (green, magnification 1000X). Contrast in both images was enhanced with ImageJ using the enhance local contrast plugin. The settings were block size = 127, histogram bins = 265, maximum slope = 3.00. **B:** Lung tissue was dual stained for TANGO1 (red) and α-SMA (green). Images are representative from two independent SSc and two independent healthy lung biopsies showing typical staining observed across all the tissues analyzed (n=12 SSc and n=8

healthy). Magnification 40X. * denotes vessel lumen; # denotes vessel neointima; bar = 5 microns

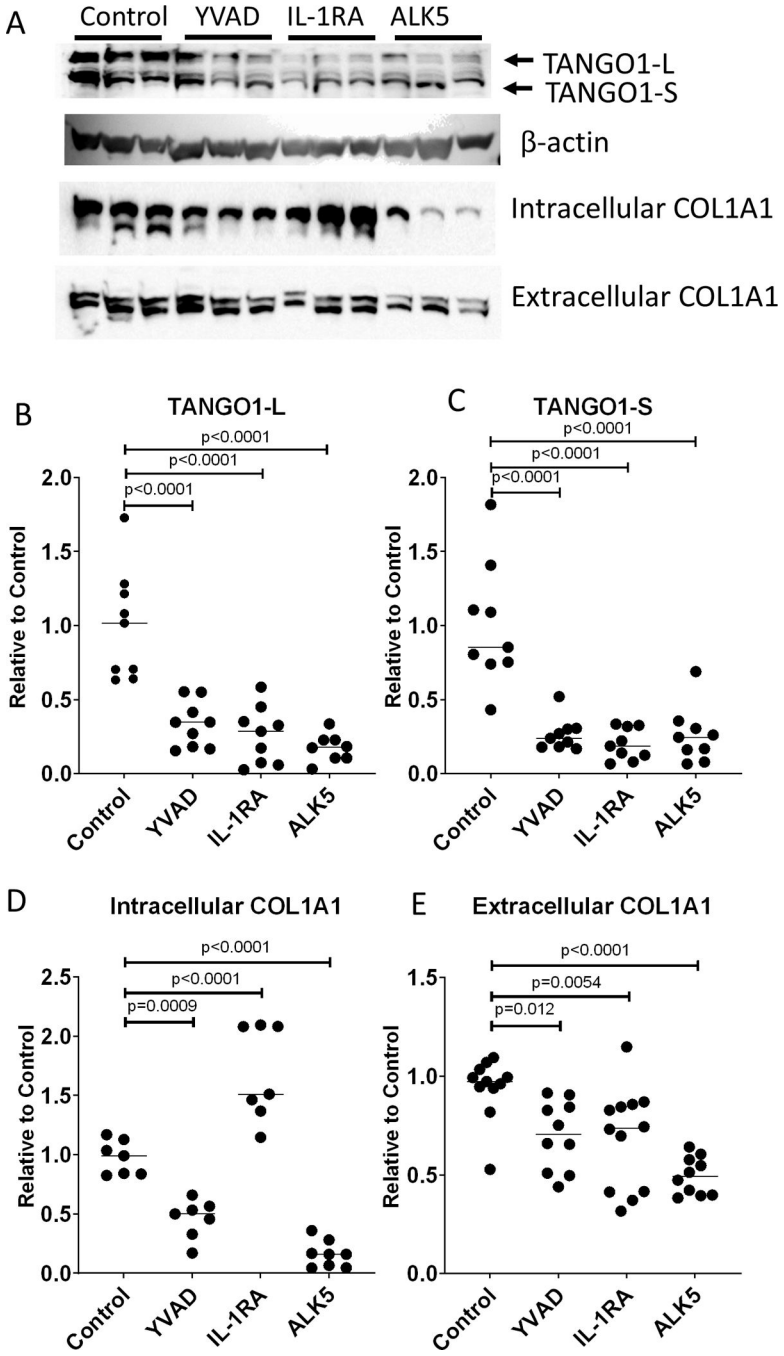

Figure 3. Inhibition of caspase-1 and its downstream signaling products reduces TANGO1 expression and lowers COL1A1 secretion.

1X10^6 SSc fibroblasts were treated with 20 μM YVAD, 2 μg/ml IL-1RA, or 10 μM ALK5 for 48 h. **A-D:** Cell lysates were assayed for TANGO1 and COL1A1 by immunoblotting and then normalized to β-actin. **E:** COL1A1 in the media was also assessed and this was normalized to total protein that had been transferred in each lane, stained with Ponceau S, (n=7–13). Data is shown as individual values in the treated groups relative to the SSc control

group. Statistical analyses: one-way ANOVA corrected with Dunnet’s multiple comparison test.

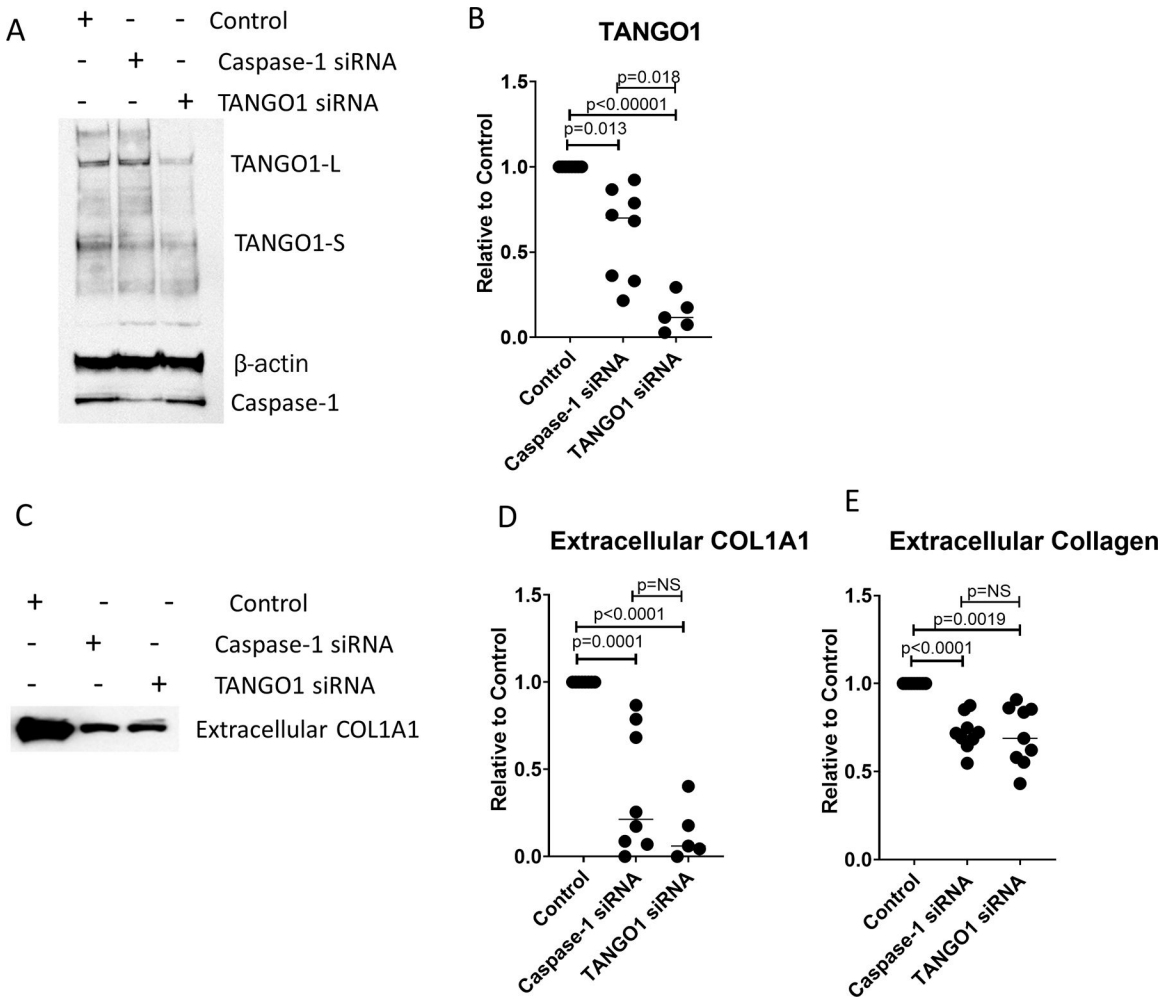

Figure 4. siRNA knockdown of caspase-1 and TANGO1 lowers secreted COL1A1 in SSc fibroblasts.

A: TANGO1 protein in caspase-1 and TANGO1 siRNA treated SSc fibroblasts. **B:** Graphical representation of TANGO1 protein from n=5–9 independent SSc fibroblast cell lines with caspase-1 siRNA or TANGO1 siRNA. **C:** Secreted COL1A1 from SSc fibroblasts with caspase-1 or TANGO1 siRNA. **D:** Graphical representation of COL1A1 protein from n=5–9 independent SSc fibroblast cell lines with caspase-1 siRNA or TANGO1 siRNA. **E:** Graphical representation of total collagen from SSc fibroblasts cell lines with caspase-1 or TANGO1 siRNA measured by sirius red (n=9). Statistical analyses: one-way ANOVA corrected with Tukey's multiple comparisons test.

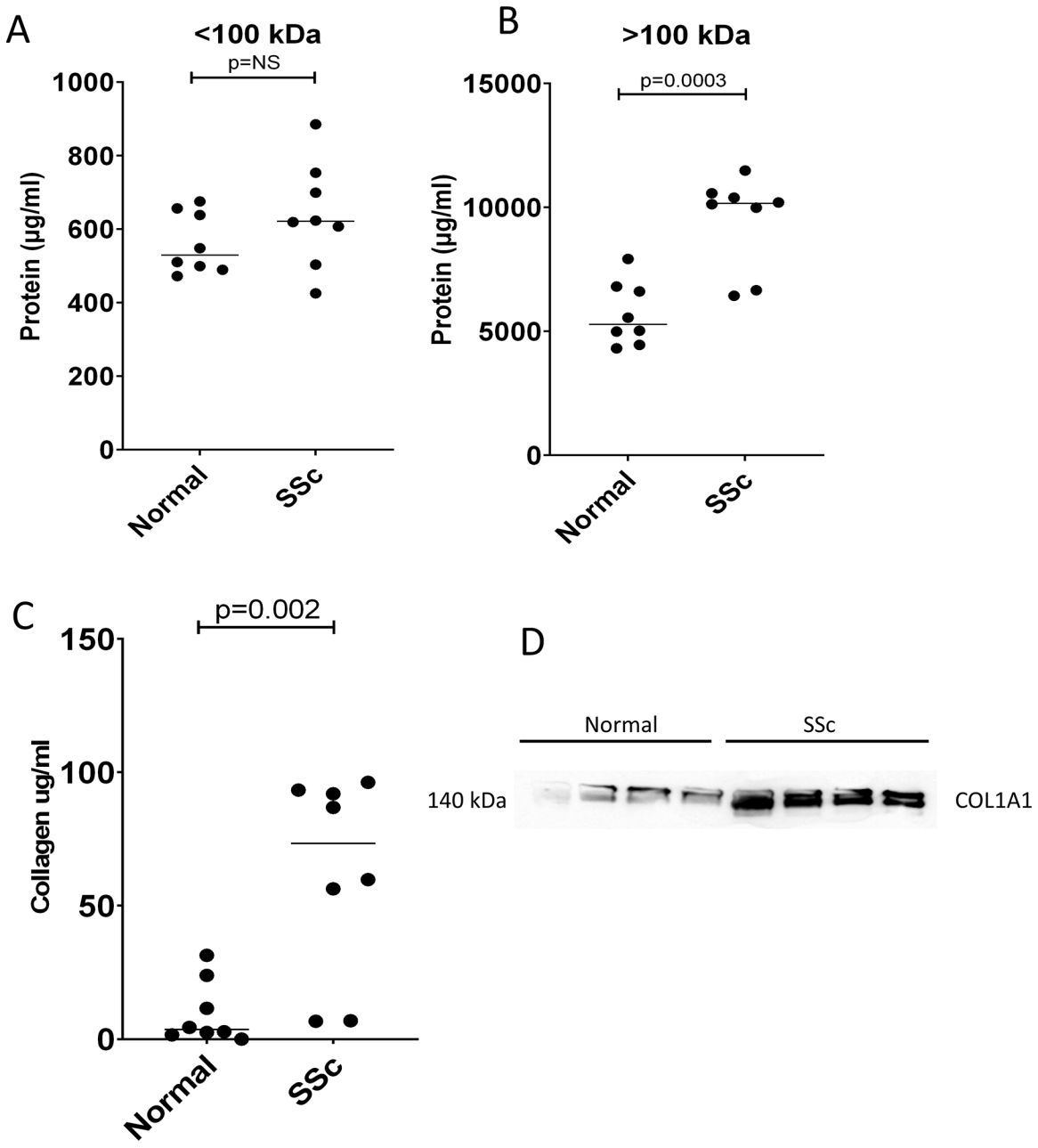

Figure 5. SSc Fibroblasts secrete more high molecular weight proteins than normal fibroblasts.

$1X10^6$ healthy or SSc fibroblasts at low passage (2–3) was cultured for 48 h and the media collected. 1 ml of the culture media was fractionated through 100 kDa cult off column. **A:** Total protein in the >100 kDa fraction, n=8 normal and n= 8 SSc. **B:** Total protein in the <100 kDa fraction, n=8 normal and n=8 SSc. **C:** Total collagen measured by sirius red in the >100 kDa fractionated samples. **D:** Immunoblots for laminin and COL1A1 from the >100 kDa fraction in n=4 normal and n=4 SSc. Individual values are demonstrated. Statistical analyses: unpaired two-tailed t-test.

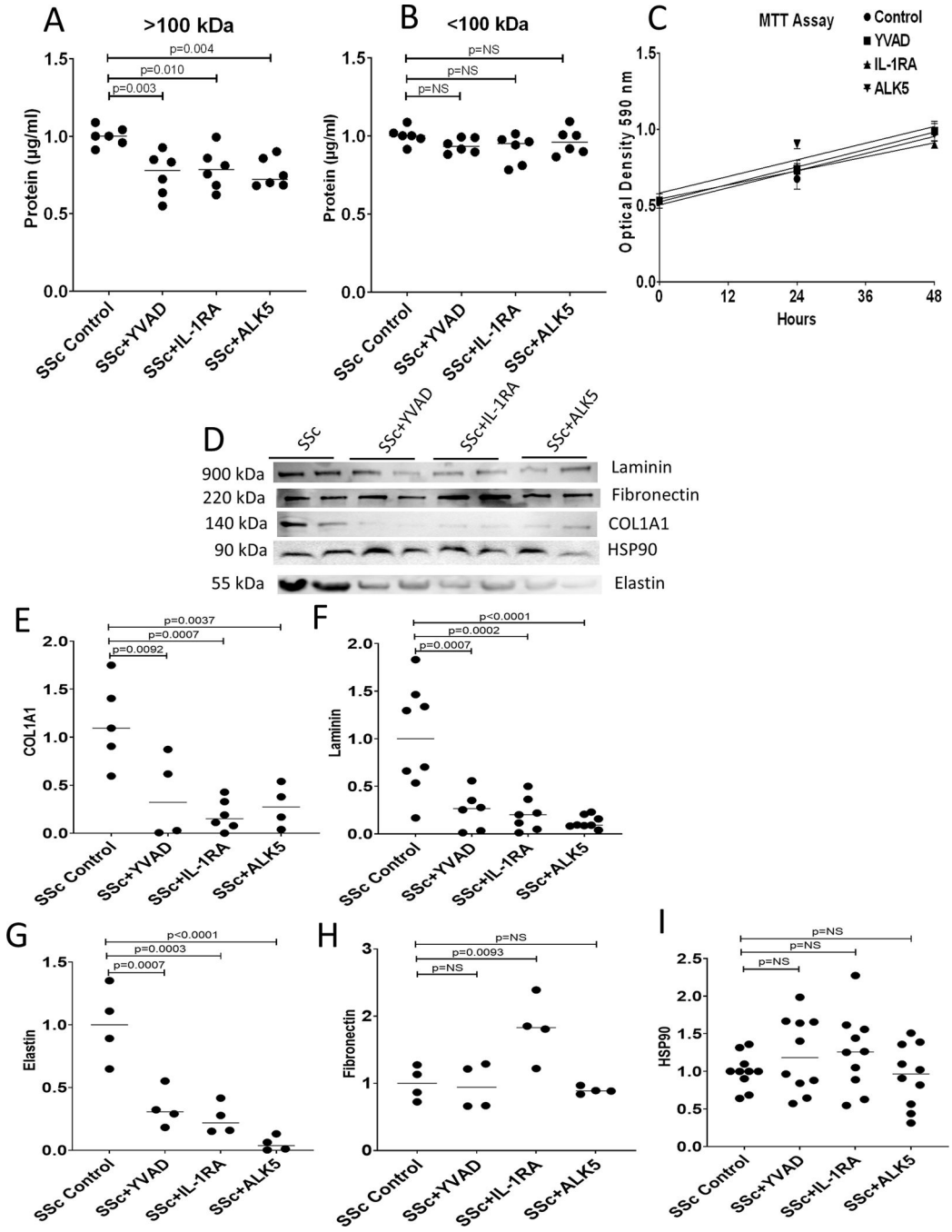

Figure 6. Reduction in TANGO1 mediated by YVAD, IL-1RA and ALK5 primarily affects large molecular weight proteins.

One milliliter of media from SSc fibroblasts presented in Figure 2 was size fractionated and assessed for protein. **A:** total protein in the > 100 kDa fraction (n=6). **B:** total protein in the < 100 kDa fraction (n=6). **C:** Fibroblast growth curve for YVAD, IL-1RA and ALK5 showing that these compounds do not promote cell death. **D:** Immunoblots for laminin, fibronectin, COL1A1, HSP90, and elastin in the fractionated samples. **E-I:** Graphical

representation of proteins from the fractionated samples (n=4–8). Statistical analyses: one-way ANOVA corrected with Dunnet's multiple comparisons test.